

Gluon fusion and $b\bar{b}$ corrections to HW^+W^-/HZZ production in the POWHEG-BOX

Julien Baglio

Institut für Theoretische Physik, Eberhard Karls Universität Tübingen, Auf der Morgenstelle 14, D-72076 Tübingen, Germany

Abstract

The study of the Higgs boson properties is one of the most important tasks to be accomplished in the next years, at the Large Hadron Collider (LHC) and at future colliders such as the Future Circular Collider in hadron-hadron mode (FCC-hh), the potential 100 TeV follow-up of the LHC machine. In this view the precise study of the Higgs couplings to weak gauge bosons is crucial and requires as much information as possible. After the recent calculation of the next-to-leading order QCD corrections to the production cross sections and differential distributions of a Standard Model Higgs boson in association with a pair of weak bosons, matched with parton shower in the POWHEG-BOX framework, we present the gluon fusion correction $gg \rightarrow HW^+W^-(HZZ)$ to the process $pp \rightarrow HW^+W^-(HZZ)$. This correction can be sizeable and amounts to +3% (+10%) in the HW^+W^- process and +5% (+18%) in the HZZ process at the LHC (FCC-hh). We also present the first study of the impact of the bottom-quark initiated channels $b\bar{b} \rightarrow HW^+W^-/HZZ$ and find that they induce a significant +18% correction in the HW^+W^- channel at the FCC-hh. We present results on total cross sections and distributions at the LHC and at the FCC-hh.

Keywords: Higgs, weak bosons, QCD corrections, LHC, FCC-hh, parton shower

1. Introduction

After the discovery of a Higgs boson with a mass of ~ 125 GeV in the Run I of the Large Hadron Collider (LHC) at CERN [1, 2], the study of its properties has begun, in particular to test whether they deviate from the predictions of the Standard Model (SM) mechanism [3–5]. The latest results at 13 TeV still display a compatibility with the SM hypothesis [6–8]. Developing the most exhaustive survey of possible deviations from the SM is thus an important task. In this view the coupling between a Higgs boson and weak bosons is a crucial part of this survey. The production of a Higgs boson in association with a pair of weak gauge bosons [9–12] can be used to probe the Higgs gauge couplings [13], which is also directly related to the triple gauge bosons vertex [14].

The next-to-leading order (NLO) QCD corrections to various $H + VV'$ processes at the LHC have now been calculated: HW^+W^- production [15–17], $HW^\pm Z$ production [16–18], associated production with a massive gauge boson W/Z and a photon [16, 19, 20], and finally HZZ production [16, 17]. The matching with parton shower for all processes was done in the MadGraph5_aMC@NLO framework in 2014 [16] (including all loop-induced gluon fusion contributions [21]) and was also completed in 2015 in the POWHEG-BOX framework [22, 23] for all processes except

those involving a photon [17]. The gluon fusion correction to HW^+W^- , $gg \rightarrow HW^+W^-$, exists in the literature [15, 21] and amounts to $\sim +4\%$ to the total cross section at the LHC for a fixed central scale. The gluon fusion correction to HZZ was calculated in Ref. [21] and amounts to +0.1 fb to the total cross section at the 13 TeV LHC for a dynamical central scale.

This Letter is a follow-up to Ref. [17] and completes the picture in the POWHEG-BOX framework by presenting the gluon fusion corrections to HW^+W^- and HZZ production in the SM and their matching with parton shower. We will also present, for the first time, a study of the impact of bottom-quark contributions in the five-flavour scheme, $pp \rightarrow b\bar{b} \rightarrow HW^+W^-/HZZ$. We find that they induce significant corrections in particular in the HW^+W^- channel. The paper is organised as follows: in Section 2 the calculation and the tools used are presented, then in Section 3 the numerical results are presented, both for the LHC and the Future Circular Collider in hadron-hadron mode (FCC-hh), the potential machine which would follow the LHC with an energy of 100 TeV. A short conclusion will be given in Section 4.

2. Description of the calculation

The leading order (LO) processes $pp \rightarrow HW^+W^-$ and $pp \rightarrow HZZ$, together with their NLO QCD corrections, have been discussed in Ref. [17]. We only discuss in this Letter the LO gluon fusion correction $pp \rightarrow gg \rightarrow HVV$

Email address: julien.baglio@uni-tuebingen.de (Julien Baglio)

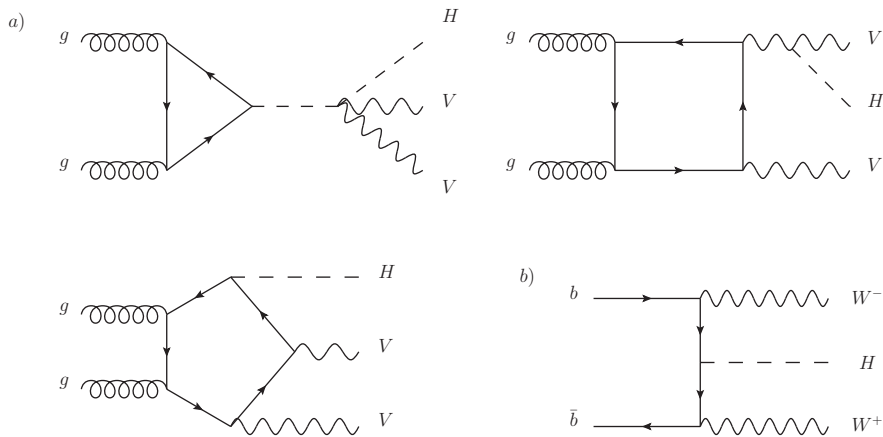


Figure 1: a) A selection of representative diagrams for $gg \rightarrow HVV$ production processes. V stands for W or Z bosons. b) LO diagram for the channel $b\bar{b} \rightarrow HW^+W^-$ with the top Yukawa coupling.

and the NLO QCD-corrected bottom-quark contribution $pp \rightarrow b\bar{b} \rightarrow HVV$ at proton-proton colliders, where VV stands either for W^+W^- or for ZZ . The gluon fusion channel is formally a next-to-next-to-leading order contribution to the full hadronic cross section $pp \rightarrow HVV$, nevertheless we will combine it with the NLO QCD calculation of the quark channels $pp \rightarrow q\bar{q} \rightarrow HVV$ as done for the W^+W^- and ZZ production processes, see for example Ref. [24] and references therein. The gluon fusion correction for the HW^+W^- process was calculated in Ref. [15] and it was shown that it has an impact of $\sim +4\%$ at $M_H = 120$ GeV for a central scale $\mu = (M_H + 2M_W)/2$. The $b\bar{b}$ channel has never been considered in the literature so far.

The $gg \rightarrow HVV$ contribution is a one-loop contribution already at the lowest order and proportional to α_s^2 . It consists of triangle, box and pentagon loops of quarks. Our calculation is done with five active massless flavours for the running of the strong coupling constant α_s , and we use diagonal Cabibbo-Kobayashi-Maskawa (CKM) matrix elements for the HW^+W^- process. Diagrams involving a Yukawa coupling between a light quark and a Higgs boson are discarded, so that in the pentagon loops only the top quark contributes. We use the 't Hooft-Feynman gauge. We depict in Fig. 1 a) some generic diagrams, in particular the pentagon class involving the quark-quark-Higgs coupling.

The full one-loop amplitude is ultraviolet (UV) and infrared (IR) finite and is convoluted with the gluon parton distribution functions (PDF) to obtain the hadronic cross section as

$$\sigma^{gg} = \int dx_1 dx_2 [g(x_1, \mu_F) g(x_2, \mu_F) \hat{\sigma}^{gg \rightarrow HVV}], \quad (1)$$

where $g(x, \mu_F)$ denotes the gluon PDF with momentum fraction x and factorisation scale μ_F . The PDF evolution is taken at NLO as well as the running of α_s . The one-loop amplitude is generated with `FeynArts-3.7` [25]

and calculated with `FormCalc-8.4` [26]. The scalar integrals as well as the reduction of tensor coefficients down to scalar integrals are calculated using the techniques developed in Refs. [27–29] and implemented with `Collier 1.0` [30], adapted to the `FormCalc` framework thanks to an in-house routine. The final code is implemented in the framework of the `POWHEG-BOX` [23]. To improve the stability of the calculation of the amplitudes a technical cut has been implemented,

$$k_{ij} \geq k_{\text{cut}}, \quad k_{ij} = \min(\tilde{k}_{ij}, p_{T,i}, p_{T,j}), \quad (2)$$

$$\tilde{k}_{ij} = \frac{3}{5} \min(p_{T,i}, p_{T,j}) \sqrt{\Delta y_{ij}^2 + \Delta \phi_{ij}^2},$$

where (ij) runs on the pairs of final-state particles ($i \neq j$), Δy_{ij} and $\Delta \phi_{ij}$ are the rapidity and angular separations between the particle i and j , $p_{T,i}$ is the transverse momentum of particle i , and $k_{\text{cut}} = 10^{-2}$. This technical cut helps to get rid of regions where the Gram determinant of the tensor integrals is close to zero, acting in much the same way as a jet veto. It has been checked that the result does not depend on the value of k_{cut} (as long as k_{cut} is small enough). Note that the calculation could be done without this cut, but at the cost of increasing the number of points in the integration routine, thus slowing down the whole calculation.

The bottom-quark contribution in the case of the HZZ channel is calculated in much the same way as in Ref. [17] for the light quark contributions, as we take the bottom quark massless and use the bottom-quark PDF in a five-flavour-scheme. The Feynman diagrams are similar and the renormalisation is the same. The calculation of the channel $pp \rightarrow b\bar{b} \rightarrow HW^+W^-$ includes one new diagram at LO, depicted in Fig. 1 b), involving the top-quark Yukawa coupling.

The real corrections at NLO in the HW^+W^- channel involve resonant diagrams with on-shell top-quark which lead to a double-counting with the production process $pp \rightarrow HW^-t$ followed by the on-shell decay $t \rightarrow W^+b$. This is-

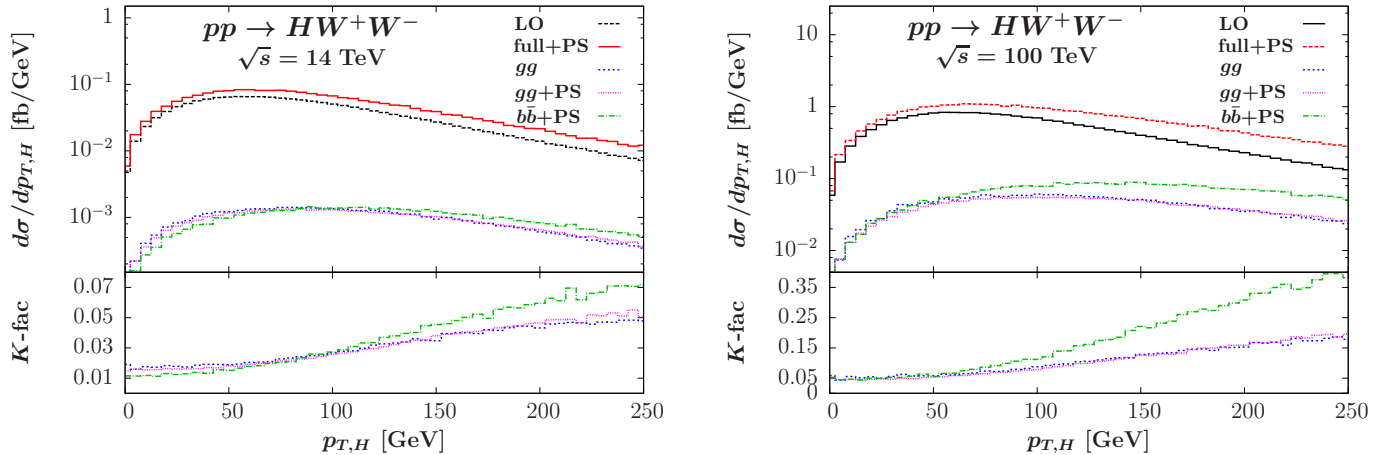


Figure 2: In the main frame: Higgs transverse momentum $p_{T,H}$ (in GeV) distribution of the $pp \rightarrow HW^+W^-$ cross section (in fb/GeV) at the 14 TeV LHC (left) and at the 100 TeV FCC-hh (right) calculated with the PDF4LHC15_nlo PDF set and with the input parameters given in Eq. (3). In black (dashed): the LO QCD distribution; in red (solid): the full distribution including NLO QCD corrections as well as the gg and $b\bar{b}$ contributions, corrected with PS effects; in blue (dotted): the gg contribution; in pink (thin dotted): the gg contribution including PS effects; in green (dash-dotted): the $b\bar{b}$ contribution including PS effects. In the insert are displayed the gg , the $gg+PS$ and the $b\bar{b}+PS$ K -factors relative to the LO prediction. The $b\bar{b}$ contribution without PS effects would be nearly the same as the curve including them.

sue is well known in W -pair production (see for example Refs. [31, 32]) and one way to solve it is to introduce a b -jet veto with a 100% efficiency as done in Ref. [31] for W -pair production. If a more realistic jet veto is wanted, a more complicated diagram subtraction method has to be used [33]. We will not enter in such details which go beyond the scope of this paper as it would not change significantly the amount of QCD corrections to the bottom-quark fusion process, which itself is a sub-leading channel of the full process $pp \rightarrow HW^+W^-$. To implement this b -jet veto we simply omit the contributions with a gluon in the initial state at the level of the PDFs.

We use the same phase-space parametrisation that was used in our previous work [17] for both gluon fusion and bottom-quark fusion contributions. It has been checked explicitly that the amplitudes are UV and IR finites. In addition, adopting the same framework as in Ref. [15] for the HW^+W^- process, a good agreement has been found between their results and our calculation.

3. Numerical results at the LHC and at the FCC

Following strictly the framework of our previous work [17], we use the following set of input parameters,

$$\begin{aligned} G_F &= 1.16637 \times 10^{-5} \text{ GeV}^{-2}, \quad M_W = 80.385 \text{ GeV}, \\ M_Z &= 91.1876 \text{ GeV}, \quad M_t = 172.5 \text{ GeV}, \\ M_H &= 125 \text{ GeV}, \quad \alpha_s^{\text{NLO}}(M_Z^2) = 0.118, \end{aligned} \quad (3)$$

where all but M_H is taken from Ref. [34]. The CKM matrix is assumed to be diagonal and the masses of all the quarks but the top quark are approximated as zero. Following the latest PDF4LHC Recommendation [35] we use in the LHAPDF6 framework [36] the NLO PDF set family PDF4LHC15_nlo which combines the three global sets

CT14 [37], MMHT14 [38] and NNPDF3.0 [39] using the combination method developed in [40, 41]. To define the jets we use FastJet [42, 43] and the parton shower is done with Pythia 6.4 [44]. The central scale is defined as the HVV invariant mass, $\mu_R = \mu_F = \mu_0$ with $\mu_0^{HWW} = M_{HW^+W^-}$, $\mu_0^{HZZ} = M_{HZZ}$. The running of α_s is done at NLO throughout the whole Letter.

Using this set of parameters we obtain at the LHC at 14 TeV a $\sim +3\%$ correction to the LO $pp \rightarrow HW^+W^-$ cross section and a $\sim +5\%$ correction to the LO $pp \rightarrow HZZ$ cross section coming from the gg contributions. At the FCC-hh at 100 TeV we obtain $\sim +10\%$ and $\sim +18\%$ corrections respectively. The correction increases, in both channels, with increasing centre-of-mass (c.m.) energies. The $b\bar{b}$ contributions are less important for the HZZ channel, leading to a $\sim +2\%$ increase at the LHC and a $\sim +7\%$ increase at the FCC-hh. The NLO QCD corrections to the $b\bar{b}$ channel itself are very small, at most $\sim +3\%$ at the FCC-hh. In contrast, the impact of the $b\bar{b}$ channel is significant in the HW^+W^- channel already at LO. The new t -channel diagram depicted in Fig. 1, together with the other diagrams belonging to the same gauge-invariant class, induces this significant contribution, in particular at the FCC-hh. The NLO QCD corrections to $b\bar{b} \rightarrow HW^+W^-$ are small, $\sim +4\%$ ($+0.3\%$) at the LHC (FCC-hh). The correction from this channel to the LO $pp \rightarrow q\bar{q} \rightarrow HW^+W^-$ process is $\sim +3\%$ at the LHC and $\sim +18\%$ at the FCC-hh. The total QCD corrections, including the NLO contributions calculated in Ref. [17], eventually amount to $\sim +33\%$ ($\sim +30\%$) for the HW^+W^- (HZZ) channel at the LHC and to $\sim +57\%$ ($\sim +42\%$) for the HW^+W^- (HZZ) channel at the FCC-hh.

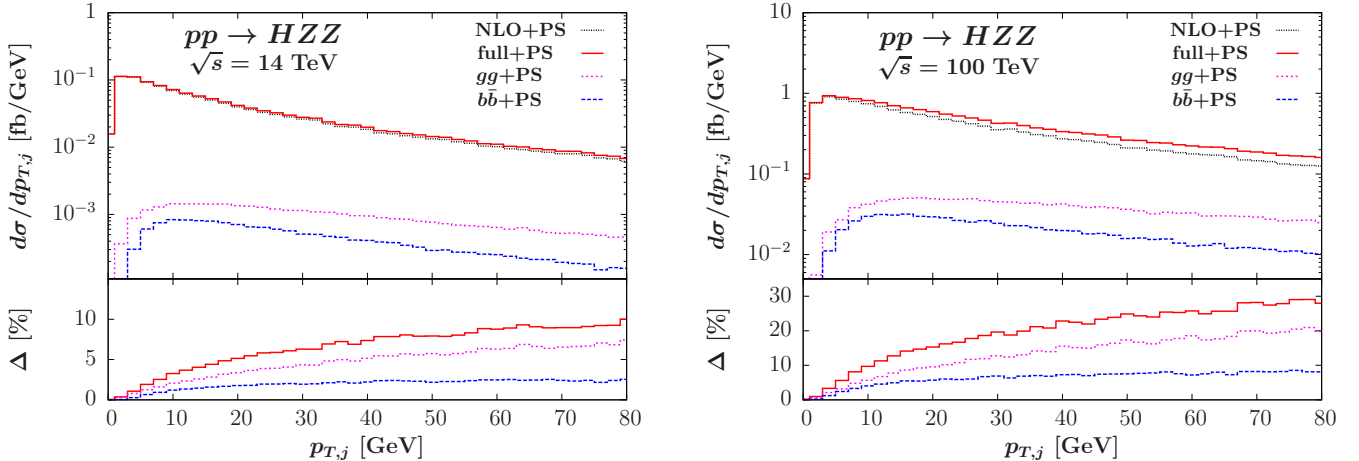


Figure 3: In the main frame: Jet transverse momentum $p_{T,j}$ (in GeV) distribution of the $pp \rightarrow HZZ$ cross section (in fb/GeV) at the 14 TeV LHC (left) and at the 100 TeV FCC-hh (right) calculated with the PDF4LHC15_nlo PDF set and with the input parameters given in Eq. (3). In black (thin dotted): the NLO distribution including PS effects; in red (solid): the full distribution including NLO QCD corrections as well as the gg and $b\bar{b}$ contributions, corrected with PS effects; in pink (dotted): the gg contribution including PS effects; in blue (dashed): the $b\bar{b}$ contribution including PS effects. In the insert are displayed the corrections Δ (in %) due to the gluon fusion and $b\bar{b}$ contributions (in pink/dotted and blue/dashed respectively) as well as their sum (in red/solid) with respect to the NLO+PS calculation.

3.1. Differential distributions

As an example of the impact of the gluon fusion and $b\bar{b}$ corrections on the differential distributions we present the Higgs transverse momentum $p_{T,H}$ for the HW^+W^- channel and the jet transverse momentum $p_{T,j}$ distributions for the HZZ channel, in both cases at the LHC and at the FCC-hh. The other kinematic distributions can be easily obtained in the POWHEG-BOX framework. Note that the distributions are quite similar between both channels, so that for example the conclusions drawn in the HW^+W^- for the $p_{T,H}$ distribution apply also in the HZZ channel, but as expected from the corrections on the total cross sections the impact of gluon fusion contributions is more visible in the HZZ channel than in the HW^+W^- channel and vice-versa for the impact of $b\bar{b}$ contributions.

In Figure 2 we display the $p_{T,H}$ distributions at the LHC (left) and the FCC-hh (right), including the LO prediction (in black/dashed line) and the full prediction including both the NLO QCD corrections and the gluon fusion and $b\bar{b}$ contributions (in red/solid line), as well as the gluon fusion contribution alone (in blue/dotted line) and with parton shower (PS) effects simulated with Pythia (in pink/thin dotted line), and finally the $b\bar{b}$ contribution including PS effects (in green/dash-dotted line). The contribution from $b\bar{b}$ subprocess alone, without PS effects, would be nearly identical to the curve including PS effects. The inserts display the K -factor of the gluon fusion and $b\bar{b}$ contributions, defined as $K = \sigma^{gg/b\bar{b}}/\sigma^{\text{LO}}$. The gg corrections are quite small at the LHC, of the order of +2% to +5%, linearly increasing from low to high $p_{T,H}$, but sizeable at the FCC-hh, from +5% to \sim +18%. The PS effects are quite small on the gg contribution but noticeable as a change in shape, leading to slightly smaller corrections at low $p_{T,H}$ and slightly larger corrections at high $p_{T,H}$. The $b\bar{b}$ effects follow the same pattern, except that

the PS effects are not significant and that the shape of the $b\bar{b}$ corrections is more quadratic. At the LHC they are of the order of +1% to +7%, smaller than gg corrections at low $p_{T,H}$ and bigger at high transverse momenta. The corrections at the FCC-hh are important, reaching \sim +40% at $p_{T,H} = 250$ GeV.

In Figure 3 we display the $p_{T,j}$ distributions at the LHC (left) and the FCC-hh (right), including the PS effects everywhere. The NLO distribution is displayed in black (thin dotted line), the full distribution including the gg and $b\bar{b}$ contributions is displayed in red (solid line), and the gg contribution as well as the $b\bar{b}$ contribution, alone, are displayed in pink (dotted line) and blue (dashed line) respectively. The insert displays the percent correction due to the gg contribution, the $b\bar{b}$ contribution as well as the sum of them, with respect to the NLO prediction. The gg contribution displays a logarithmic increase with increasing $p_{T,j}$, and is modest at the LHC but sizeable at the FCC-hh. The $b\bar{b}$ contributions are negligible for low $p_{T,j}$ and then are flat, of the order of \sim +2.5% at the LHC and \sim +9% at the FCC-hh. The sum of the two contributions reach, at high $p_{T,j}$, +10% at the LHC and +30% at the FCC-hh.

3.2. Total cross sections including theoretical uncertainties

As already demonstrated in Ref. [17] the total rates $pp \rightarrow HW^+W^-/HZZ$ are affected by theoretical uncertainties: 1) the scale uncertainty reflecting the confidence given to the calculation at a given perturbative order, calculated by varying the renormalisation scale μ_R and the factorisation scale μ_F in the range $\frac{1}{2}\mu_0 \leq \mu_R, \mu_F \leq 2\mu_0$; 2) the PDF+ α_s uncertainty reflecting the impact of the

experimental uncertainties on the fit leading to the determination of the PDFs. We calculate the theoretical uncertainties on the gluon fusion and the $b\bar{b}$ contribution as well as on their combination with the NLO QCD $q\bar{q}$ contribution to the whole hadronic cross section, following Ref. [17].

The results are presented in Tables 1 and 2 as well as displayed in Figure 4. The scale uncertainty of the gluon fusion cross sections is quite large, of the order of 15% to 30%. This was expected as this is a LO process. The scale uncertainties of the subprocess $b\bar{b} \rightarrow HW^+W^-$ are also quite large, due to the b -jet veto that we use and is mainly driven by the variation of the factorisation scale. We have checked that if a similar jet veto were used for the light-quark contributions the scale uncertainty would also rise and reach for example $\sim \pm 10\%$ at the FCC-hh instead of the $\sim \pm 4\%$ uncertainty quoted in Ref. [17]. In the case of the $b\bar{b} \rightarrow HZZ$ subprocess the scale uncertainty is slightly larger than in Ref. [17] for the light quark contributions.

The combination of the gluon fusion and $b\bar{b}$ channels with the NLO $q\bar{q}$ cross section, however, displays limited uncertainties albeit larger than for the $q\bar{q}$ channel alone, because of the sizeable impact of the gg correction in the HZZ channel and the $b\bar{b}$ correction in the HW^+W^- channel, in particular at the FCC-hh. The PDF+ α_s uncertainty is nearly the same in the $q\bar{q}$ contributions and in the full cross sections. We obtain a total theoretical uncertainty of $\sim \pm 4\%$ ($\sim \pm 9\%$) at the LHC (FCC-hh) for the HW^+W^- channel, compared to $\sim \pm 4\%$ ($\sim +6\% / -7\%$) for the NLO QCD $q\bar{q}$ contributions only [17]. In the case of the HZZ channel we obtain a total theoretical uncertainty of $\sim \pm 4\%$ ($+7\% / -8\%$) at the LHC (FCC-hh), compared to $\sim \pm 4\%$ ($+5\% / -7\%$) for the NLO QCD $q\bar{q}$ contributions only [17]. The impact of the gluon fusion and $b\bar{b}$ contributions uncertainties are then negligible at LHC energies but noticeable at the FCC-hh. Note that in comparison with Ref. [17] the HZZ channel dominates over the HW^-Z channel not only at lower c.m. energies but also at higher c.m. energies, when the gluon fusion and the $b\bar{b}$ corrections are included.

4. Conclusion

We have completed in this Letter the current picture of the QCD corrections to HW^+W^- and HZZ productions at hadron colliders in the POWHEG-BOX framework, including the matching with parton shower, by calculating the gluon fusion corrections $gg \rightarrow HW^+W^-/HZZ$ and the bottom quark fusion corrections $b\bar{b} \rightarrow HW^+W^-$. The latter are studied in this Letter for the first time and their NLO QCD corrections are also included. The gluon fusion contributions are sizeable, from $\sim +5\%$ at LHC energies up to $\sim +18\%$ at 100 TeV. The $b\bar{b}$ contributions are particularly important at the FCC-hh in the HW^+W^- channel, where they reach $\sim +18\%$. Combining the NLO corrections to the $pp \rightarrow q\bar{q} \rightarrow HW^+W^-/HZZ$ cross sections

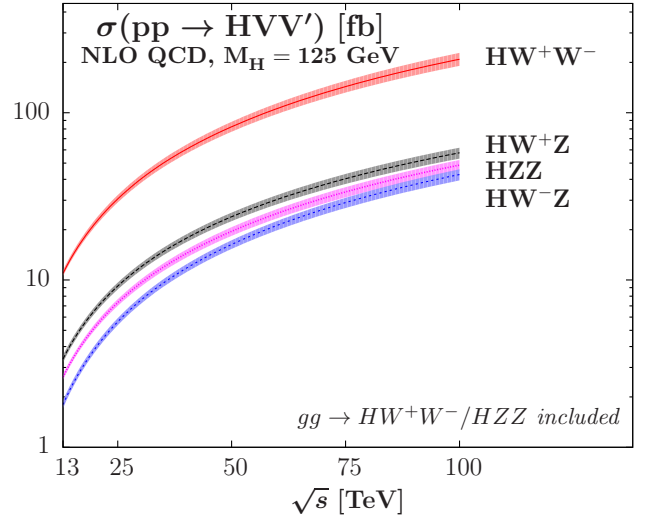


Figure 4: The total cross sections (in fb) for SM Higgs production in association with a pair of weak bosons at NLO QCD as a function of the c.m. energy (in TeV) with $M_H = 125$ GeV: HW^+W^- (red/full), HW^+Z (grey/dashed), HW^-Z (pink/dotted) and HZZ (blue/dashed with small dashes). The gluon fusion and $b\bar{b}$ contributions are included in the HW^+W^- and HZZ production channels. The PDF4LHC2015_30 PDF set has been used and the total theoretical uncertainties are included as corresponding bands around the central values. The data for the WZ channels comes from Ref. [17].

Table 1: The total HW^+W^- production cross section at the LHC and at the FCC-hh (in fb) for given c.m. energies (in TeV) at the central scale $\mu_F = \mu_R = M_{HWW}$. The first group of lines displays the $gg \rightarrow HW^+W^-$ contribution, the second group displays the $b\bar{b} \rightarrow HW^+W^-$ contribution and the third displays the combination of these contributions with the NLO QCD $q\bar{q}$ contribution taken from Ref. [17]. The corresponding shifts due to the theoretical uncertainties coming from scale variation, PDF+ α_s errors as well as the total uncertainty, when all errors are added linearly, are also shown (in %).

\sqrt{s} [TeV]	σ_{HWW}^{gg} [fb]	Scale	PDF+ α_s	Total
13	0.217	+27% -21%	+4.2% -4.2%	+31% -25%
14	0.262	+26% -20%	+3.5% -3.5%	+30% -24%
33	1.81	+21% -16%	+2.4% -2.4%	+23% -18%
100	13.8	+22% -18%	+2.2% -2.2%	+24% -20%
\sqrt{s} [TeV]	$\sigma_{HWW}^{b\bar{b}}$ [fb]	Scale	PDF+ α_s	Total
13	0.236	+22% -18%	+7.8% -7.8%	+30% -26%
14	0.293	+22% -18%	+7.6% -7.6%	+30% -25%
33	2.63	+24% -19%	+5.7% -5.7%	+29% -24%
100	24.5	+27% -20%	+4.1% -4.1%	+31% -24%
\sqrt{s} [TeV]	$\sigma_{HWW}^{\text{full}}$ [fb]	Scale	PDF+ α_s	Total
13	11.0	+2.7% -1.9%	+1.7% -1.7%	+4.4% -3.7%
14	12.4	+2.8% -2.1%	+1.7% -1.7%	+4.5% -3.8%
33	45.9	+4.5% -4.0%	+1.5% -1.5%	+6.0% -5.5%
100	209	+7.2% -6.9%	+1.9% -1.9%	+9.1% -8.7%

Table 2: Same as Table 1 but for the HZZ channel at the central scale $\mu_F = \mu_R = M_{HZZ}$.

\sqrt{s} [TeV]	σ_{HZZ}^{gg} [fb]	Scale	PDF+ α_s	Total
13	0.093	+27 % -20 %	+3.2 % -3.2 %	+31 % -23 %
14	0.113	+27 % -20 %	+3.2 % -3.2 %	+30 % -23 %
33	0.783	+20 % -16 %	+2.2 % -2.2 %	+22 % -18 %
100	6.02	+22 % -18 %	+2.1 % -2.1 %	+24 % -20 %
\sqrt{s} [TeV]	$\sigma_{HZZ}^{b\bar{b}}$ [fb]	Scale	PDF+ α_s	Total
13	0.036	+4.5 % -4.7 %	+8.0 % -8.0 %	+13 % -13 %
14	0.044	+4.4 % -4.8 %	+7.8 % -7.8 %	+12 % -13 %
33	0.323	+4.2 % -5.2 %	+5.9 % -5.9 %	+10 % -11 %
100	2.49	+3.7 % -6.5 %	+4.8 % -4.8 %	+8.5 % -11 %
\sqrt{s} [TeV]	$\sigma_{HZZ}^{\text{full}}$ [fb]	Scale	PDF+ α_s	Total
13	2.63	+2.4 % -1.8 %	+1.8 % -1.8 %	+4.2 % -3.7 %
14	2.98	+2.4 % -2.0 %	+1.7 % -1.7 %	+4.2 % -3.7 %
33	11.0	+3.4 % -3.5 %	+1.6 % -1.6 %	+5.1 % -5.1 %
100	48.6	+5.1 % -5.9 %	+2.1 % -2.1 %	+7.2 % -8.0 %

already calculated in Ref. [17] with the two new contributions studied in this Letter, the QCD corrections amounts to +33 % (+57 %) and +30 % (+42 %) for the total cross sections $pp \rightarrow HW^+W^-$ and $pp \rightarrow HZZ$ at the LHC (FCC-hh), respectively. The total theoretical uncertainty is nearly unmodified at LHC energies while the change is noticeable at the FCC-hh, from $\sim +6\% / -7\%$ to $\sim \pm 9\%$ for the HW^+W^- channel and from $\sim +5\% / -7\%$ to $\sim +7\% / -8\%$ for the HZZ channel. The impact of the gluon fusion and $b\bar{b}$ channels on the differential distributions matched to parton shower is found small at the LHC and sizeable at the FCC-hh, following the pattern of the corrections on the total cross sections. A public release of the code in the POWHEG-BOX is expected in the near future.

Acknowledgments

The author thanks Juraj Streicher and Nadège Bernard for their reading of the manuscript as well as Valentin Hirschi and Barbara Jäger for discussions. The referee is also acknowledged for his suggestion to study the $b\bar{b}$ contributions. This work was performed thanks to the support of the state of Baden-Württemberg through bwHPC and the German Research Foundation (DFG) through grant no INST 39/963-1 FUGG. The author was supported in part by the Institutional Strategy of the University of Tübingen (DFG, ZUK 63) and the DFG Grant JA 1954/1.

References

- [1] G. Aad, et al., Phys.Lett. B716 (2012) 1–29. [arXiv:1207.7214](#), [doi:10.1016/j.physletb.2012.08.020](#).
- [2] S. Chatrchyan, et al., Phys.Lett. B716 (2012) 30–61. [arXiv:1207.7235](#), [doi:10.1016/j.physletb.2012.08.021](#).
- [3] P. W. Higgs, Phys.Lett. 12 (1964) 132–133. [doi:10.1016/0031-9163\(64\)91136-9](#).
- [4] P. W. Higgs, Phys.Rev.Lett. 13 (1964) 508–509. [doi:10.1103/PhysRevLett.13.508](#).
- [5] G. Guralnik, C. Hagen, T. Kibble, Phys.Rev.Lett. 13 (1964) 585–587. [doi:10.1103/PhysRevLett.13.585](#).
- [6] ATLAS Collaboration, ATLAS-CONF-2016-081 (2016). URL <https://cds.cern.ch/record/2206272>
- [7] CMS Collaboration, CMS-PAS-HIG-16-020 (2016). URL <https://cds.cern.ch/record/2205275>
- [8] CMS Collaboration, CMS-PAS-HIG-16-033 (2016). URL <https://cds.cern.ch/record/2204926>
- [9] M. Baillargeon, F. Boudjema, F. Cuyper, E. Gabrielli, B. Mele, Nucl.Phys. B424 (1994) 343–373. [arXiv:hep-ph/9307225](#), [doi:10.1016/0550-3213\(94\)90298-4](#).
- [10] K.-m. Cheung, Phys.Rev. D49 (1994) 6224–6227. [doi:10.1103/PhysRevD.49.6224](#).
- [11] A. Djouadi, Phys.Rept. 457 (2008) 1–216. [arXiv:hep-ph/0503172](#), [doi:10.1016/j.physrep.2007.10.004](#).
- [12] J. Baglio, A. Djouadi, J. Quevillon, Rep. Prog. Phys. 79 (11) (2016) 116201. [arXiv:1511.07853](#), [doi:10.1088/0034-4885/79/11/116201](#).
- [13] E. Gabrielli, M. Heikinheimo, L. Marzola, B. Mele, C. Spethmann, et al., Phys.Rev. D89 (5) (2014) 053012. [arXiv:1312.4956](#), [doi:10.1103/PhysRevD.89.053012](#).
- [14] T. Corbett, O. Éboli, J. Gonzalez-Fraile, M. Gonzalez-Garcia, Phys.Rev.Lett. 111 (2013) 011801. [arXiv:1304.1151](#), [doi:10.1103/PhysRevLett.111.011801](#).
- [15] S. Mao, M. Wen-Gan, Z. Ren-You, G. Lei, W. Shao-Ming, et al., Phys.Rev. D79 (2009) 054016. [arXiv:0903.2885](#), [doi:10.1103/PhysRevD.79.054016](#).
- [16] J. Alwall, R. Frederix, S. Frixione, V. Hirschi, F. Maltoni, O. Mattelaer, H. S. Shao, T. Stelzer, P. Torrielli, M. Zaro, JHEP 07 (2014) 079. [arXiv:1405.0301](#), [doi:10.1007/JHEP07\(2014\)079](#).
- [17] J. Baglio, Phys. Rev. D93 (5) (2016) 054010. [arXiv:1512.05787](#), [doi:10.1103/PhysRevD.93.054010](#).
- [18] N. Liu, J. Ren, B. Yang, Phys.Lett. B731 (2014) 70–73. [arXiv:1310.6192](#), [doi:10.1016/j.physletb.2014.02.023](#).
- [19] S. Mao, W. Neng, L. Gang, M. Wen-Gan, Z. Ren-You, et al., Phys. Rev. D88 (2013) 076002. [arXiv:1310.0946](#), [doi:10.1103/PhysRevD.88.076002](#).
- [20] X. Shou-Jian, M. Wen-Gan, G. Lei, Z. Ren-You, C. Chong, et al., J.Phys. G42 (6) (2015) 065006. [arXiv:1505.03226](#), [doi:10.1088/0954-3899/42/6/065006](#).
- [21] V. Hirschi, O. Mattelaer, JHEP 10 (2015) 146. [arXiv:1507.00020](#), [doi:10.1007/JHEP10\(2015\)146](#).
- [22] S. Frixione, P. Nason, C. Oleari, JHEP 0711 (2007) 070. [arXiv:0709.2092](#), [doi:10.1088/1126-6708/2007/11/070](#).
- [23] S. Alioli, P. Nason, C. Oleari, E. Re, JHEP 1006 (2010) 043. [arXiv:1002.2581](#), [doi:10.1007/JHEP06\(2010\)043](#).
- [24] J. M. Campbell, R. K. Ellis, C. Williams, JHEP 1107 (2011) 018. [arXiv:1105.0020](#), [doi:10.1007/JHEP07\(2011\)018](#).
- [25] T. Hahn, Comput.Phys.Commun. 140 (2001) 418–431. [arXiv:hep-ph/0012260](#), [doi:10.1016/S0010-4655\(01\)00290-9](#).
- [26] T. Hahn, M. Perez-Victoria, Comput.Phys.Commun. 118 (1999) 153–165. [arXiv:hep-ph/9807565](#), [doi:10.1016/S0010-4655\(98\)00173-8](#).
- [27] A. Denner, S. Dittmaier, Nucl. Phys. B658 (2003) 175–202. [arXiv:hep-ph/0212259](#), [doi:10.1016/S0550-3213\(03\)00184-6](#).
- [28] A. Denner, S. Dittmaier, Nucl. Phys. B734 (2006) 62–115. [arXiv:hep-ph/0509141](#), [doi:10.1016/j.nuclphysb.2005.11.007](#).
- [29] A. Denner, S. Dittmaier, Nucl. Phys. B844 (2011) 199–242. [arXiv:1005.2076](#), [doi:10.1016/j.nuclphysb.2010.11.002](#).
- [30] A. Denner, S. Dittmaier, L. Hofer, [arXiv:1604.06792](#).

- [31] A. Bierweiler, T. Kasprzik, J. H. Kühn, S. Uccirati, JHEP 11 (2012) 093. [arXiv:1208.3147](#), [doi:10.1007/JHEP11\(2012\)093](#).
- [32] J. Baglio, L. D. Ninh, M. M. Weber, Phys.Rev. D88 (2013) 113005. [arXiv:1307.4331](#), [doi:10.1103/PhysRevD.88.113005](#); J. Baglio, L. D. Ninh, M. M. Weber, Phys.Rev. D94 (2016) 099902 (Erratum), [doi:10.1103/PhysRevD.94.099902](#).
- [33] T. Gehrmann, M. Grazzini, S. Kallweit, P. Maierhöfer, A. von Manteuffel, S. Pozzorini, D. Rathlev, L. Tancredi, Phys. Rev. Lett. 113 (21) (2014) 212001. [arXiv:1408.5243](#), [doi:10.1103/PhysRevLett.113.212001](#).
- [34] K. A. Olive, et al., Chin. Phys. C38 (2014) 090001. [doi:10.1088/1674-1137/38/9/090001](#).
- [35] J. Butterworth, et al., J. Phys. G43 (2016) 023001. [arXiv:1510.03865](#), [doi:10.1088/0954-3899/43/2/023001](#).
- [36] A. Buckley, J. Ferrando, S. Lloyd, K. Nordström, B. Page, M. Rüfenacht, M. Schönherr, G. Watt, Eur. Phys. J. C75 (2015) 132. [arXiv:1412.7420](#), [doi:10.1140/epjc/s10052-015-3318-8](#).
- [37] S. Dulat, T.-J. Hou, J. Gao, M. Guzzi, J. Huston, P. Nadolsky, J. Pumplin, C. Schmidt, D. Stump, C. P. Yuan, Phys. Rev. D93 (3) (2016) 033006. [arXiv:1506.07443](#), [doi:10.1103/PhysRevD.93.033006](#).
- [38] L. A. Harland-Lang, A. D. Martin, P. Motylinski, R. S. Thorne, Eur. Phys. J. C75 (5) (2015) 204. [arXiv:1412.3989](#), [doi:10.1140/epjc/s10052-015-3397-6](#).
- [39] R. D. Ball, et al., JHEP 04 (2015) 040. [arXiv:1410.8849](#), [doi:10.1007/JHEP04\(2015\)040](#).
- [40] J. Gao, P. Nadolsky, JHEP 07 (2014) 035. [arXiv:1401.0013](#), [doi:10.1007/JHEP07\(2014\)035](#).
- [41] S. Carrazza, S. Forte, Z. Kassabov, J. I. Latorre, J. Rojo, Eur. Phys. J. C75 (8) (2015) 369. [arXiv:1505.06736](#), [doi:10.1140/epjc/s10052-015-3590-7](#).
- [42] M. Cacciari, G. P. Salam, Phys. Lett. B641 (2006) 57–61. [arXiv:hep-ph/0512210](#), [doi:10.1016/j.physletb.2006.08.037](#).
- [43] M. Cacciari, G. P. Salam, G. Soyez, Eur. Phys. J. C72 (2012) 1896. [arXiv:1111.6097](#), [doi:10.1140/epjc/s10052-012-1896-2](#).
- [44] T. Sjöstrand, S. Mrenna, P. Z. Skands, JHEP 05 (2006) 026. [arXiv:hep-ph/0603175](#), [doi:10.1088/1126-6708/2006/05/026](#).